Short wavelength fluctuations in the solar wind

***Stuart D. Bale**, Physics Dept and SSL, University of California, Berkeley*

My Collaborators: S. Kilpua, K. Xu, C. Salem, J. C. Kasper, G. G. Howes, and E. Quataert

Center for Magnetic Self-Organization, General Meeting, June 2008

outline

- what's happening at short wavelengths (kρ ~ 1) in the solar wind? a secondary cascade? local instabilities? current sheets?
- Cluster spacecraft measurements of δE and δB at around 1 Hz suggest kinetic Alfven waves
- Measurements in the magnetosheath show copious reconnecting current sheets
- Wind/MFI measurements of magnetic fluctuation power and compressibility and association with proton anisotropy
- Relationship to the measured magnetic power spectrum
- Wind/3DP measurements of electron anisotropies - constraint on the halo anisotropies

Short wavelength e/m field measurements

- Electric field measurements
- (PI) Magnetic noise levels:
  - ~10^{-4} nT^2/Hz Cluster
  - ~10^{-6} nT^2/Hz Wind
    - core noise
    - electronics and SC noise
    - ‘interrupt-driving processing’

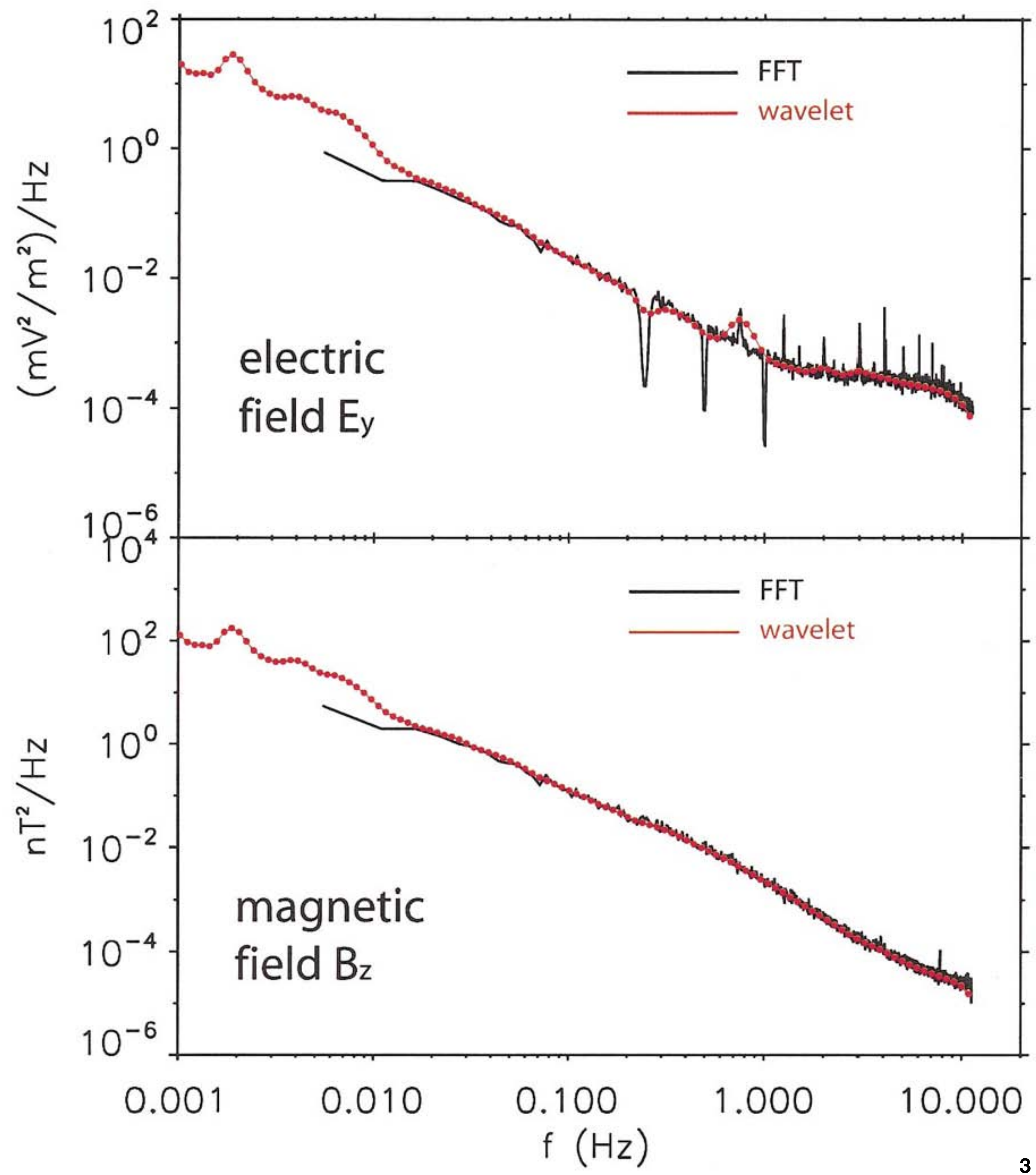

Short wavelength electric field measurements

- Cluster EFW + FGM measurements in the solar wind
- E_y and B_z with v_{sw} removed
- E_y/B_z shows simple dispersion, as KAW
- E and B are correlated (and coherent) up to $k\rho \sim 3$

Bale et al (2005)

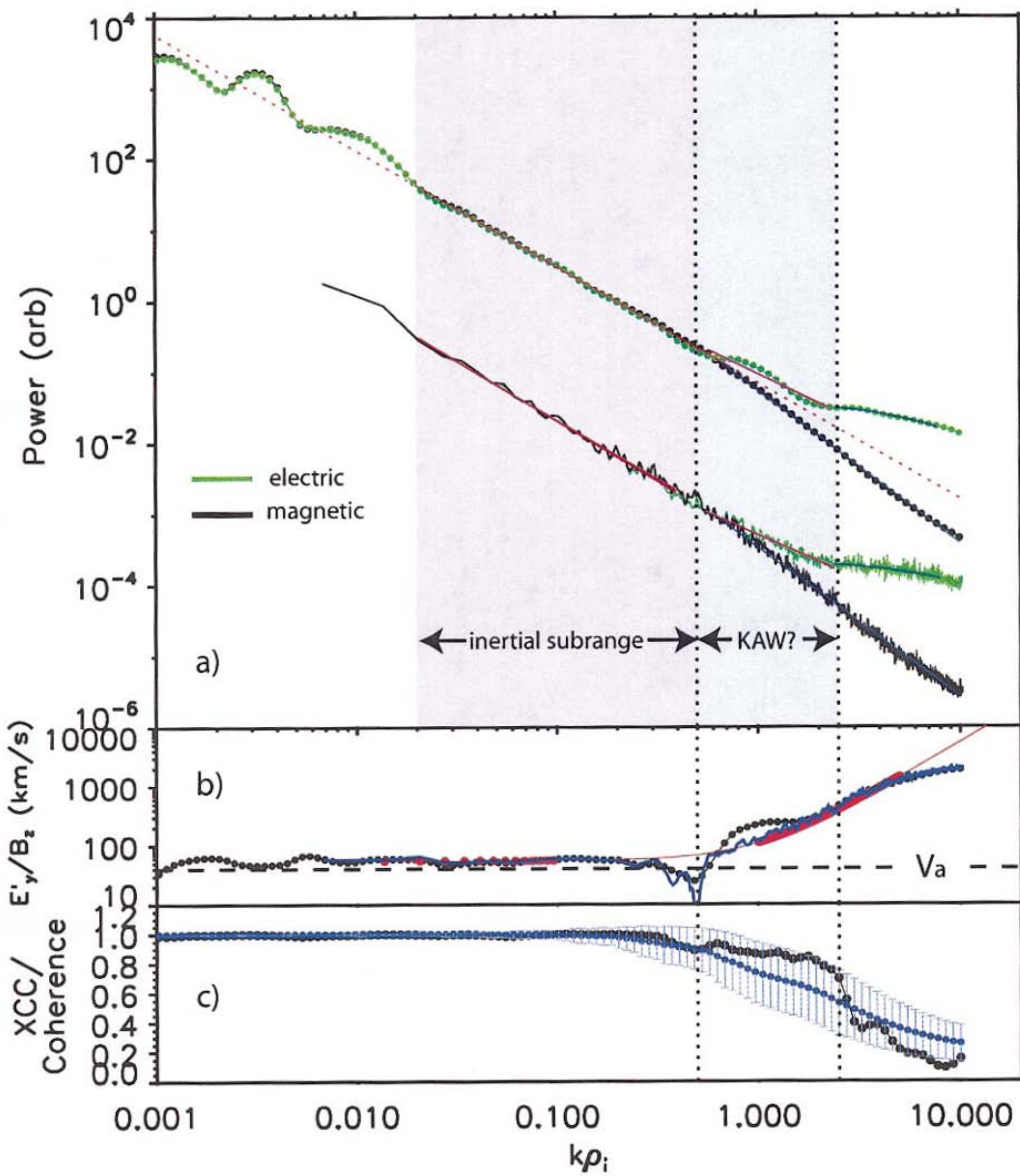

Short wavelength electric field measurements

Table 3. Values of relevant solar wind parameters, breakpoint values, spectral indices and fit parameter v_0

Time Interval	V_{sw} (km/s)	B (nT)	β	M_A	V_A (km/s)	v_0	χ^2	$k\rho_b$	S1	S2	S3
2001/02/22 15:00-17:00	365	5.2	0.42	7.9	46.1	49.3	8.8	0.16	1.70	3.01	2.10
2003/01/30 03:00-05:00	458	12.1	0.17	5.0	91.2	36.1	2.2	0.17	1.70	3.55	2.68
2003/02/13 10:30-14:30	382	10.5	0.26	6.9	55.5	38.6	1.5	0.21	1.70	3.16	1.27
2003/03/11 04:00-06:00	423	6.1	0.50	9.6	44.2	46.6	2.1	0.24	1.71	3.36	2.74
2003/03/11 09:00-11:00	426	7.8	0.41	7.8	54.5	43.9	1.9	0.21	1.70	3.53	2.60
2003/03/25 08:30-10:30	425	4.4	0.24	10.2	41.6	51.4	2.5	0.19	1.69	2.90	1.29
2003/03/30 01:30-04:30	434	11.9	0.30	6.8	63.3	61.2	0.7	0.31	1.80	2.85	1.77
2004/01/22 06:00-08:00	633	16.3	1.07	7.6	82.9	85.1	1.1	0.80	1.80	3.22	2.20
2004/01/27 00:00-02:00	468	9.6	0.24	5.9	79.2	51.4	1.3	0.21	1.60	3.19	2.12
2004/02/09 12:30-14:30	399	5.5	0.44	7.3	54.8	52.1	1.3	0.22	1.70	3.03	2.21
2004/02/22 02:00-05:00	379	8.0	0.30	5.4	70.3	34.0	0.4	0.29	1.55	3.27	2.90
2004/02/22 06:00-08:00	378	8.4	0.22	5.9	63.8	27.1	3.9	0.19	1.55	3.11	2.77
2004/03/05 00:30-03:00	462	5.0	0.13	7.9	58.2	62.9	2.4	0.12	1.75	2.45	1.15
2004/04/23 12:30-14:30	437	6.9	1.05	10.3	42.5	55.2	1.8	0.59	1.70	3.06	1.20

- 14 intervals
- S1 = 5/3 mostly
- S2 ~ (2-4)
- S3 ~ (1-3)
- good fits to ‘KAW’ phase speed
- some scaling with beta

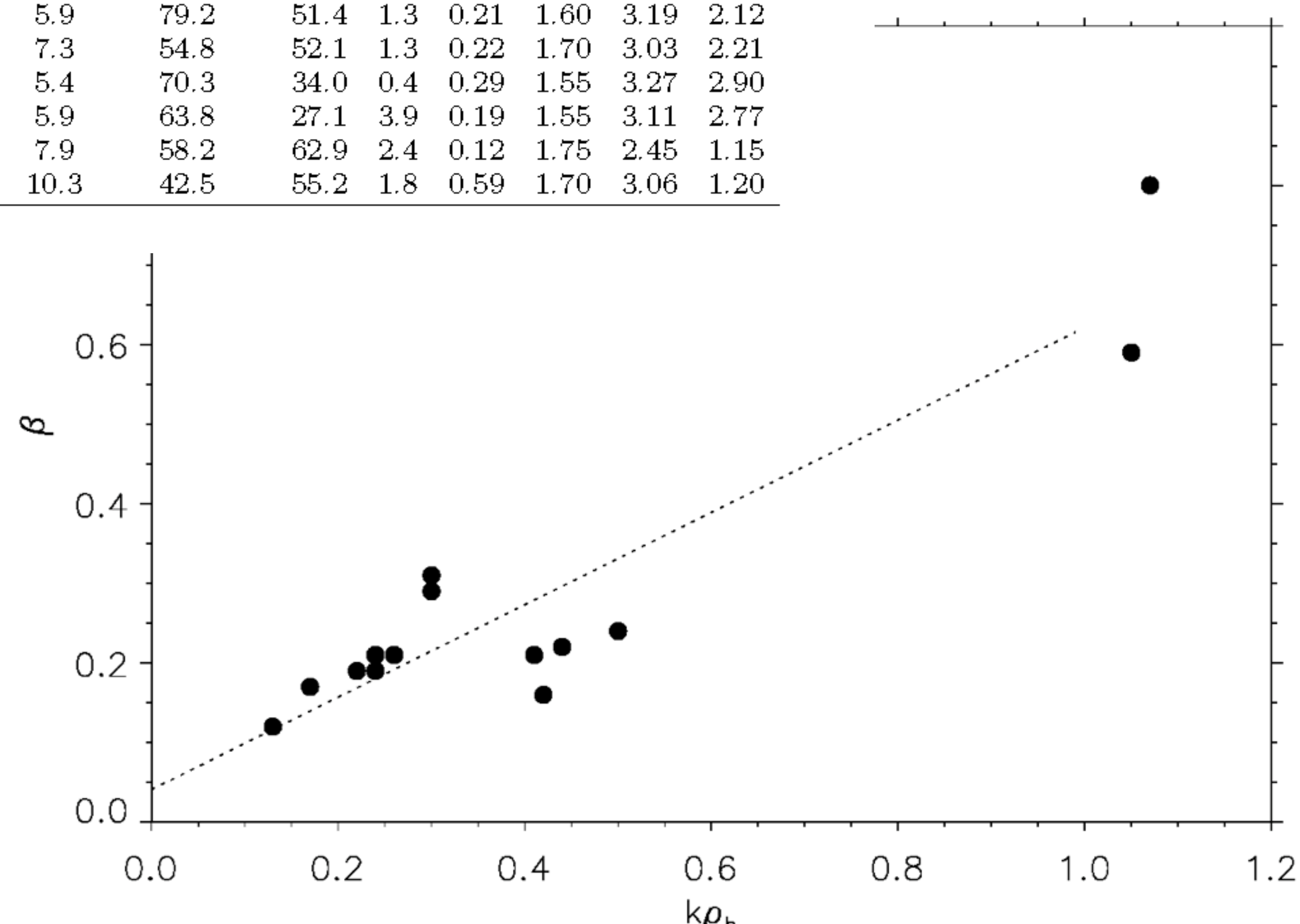

Shorter wavelength e/m measurements

- Cluster FGM/EFW/STAFF results
- Magnetic power hits the SCM noise floor generally before f_{ce}
- Intercalibration issues...

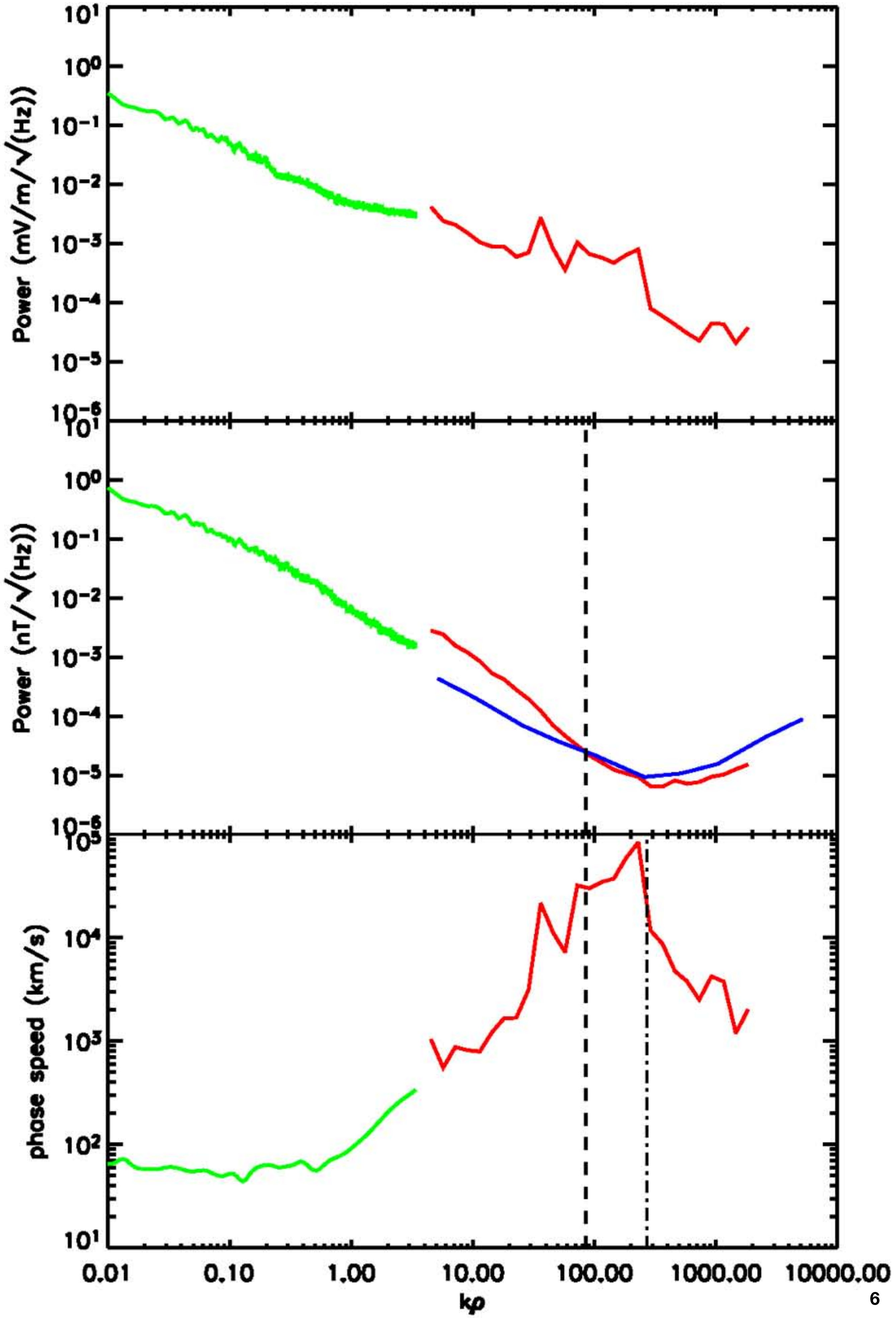

small-scale current sheets

- L ~ 3-5 c/ω_{pi}
- terrestrial magnetosheath
- prefers $Q_{||}$ geometry
- high β (β > 5)
- produce a steepened PSD above the ‘inertial’ range (which is modified in the magnetosheath)
- similar results in the solar wind (work in progress)

(Sundkvist et al., PRL, 2006)

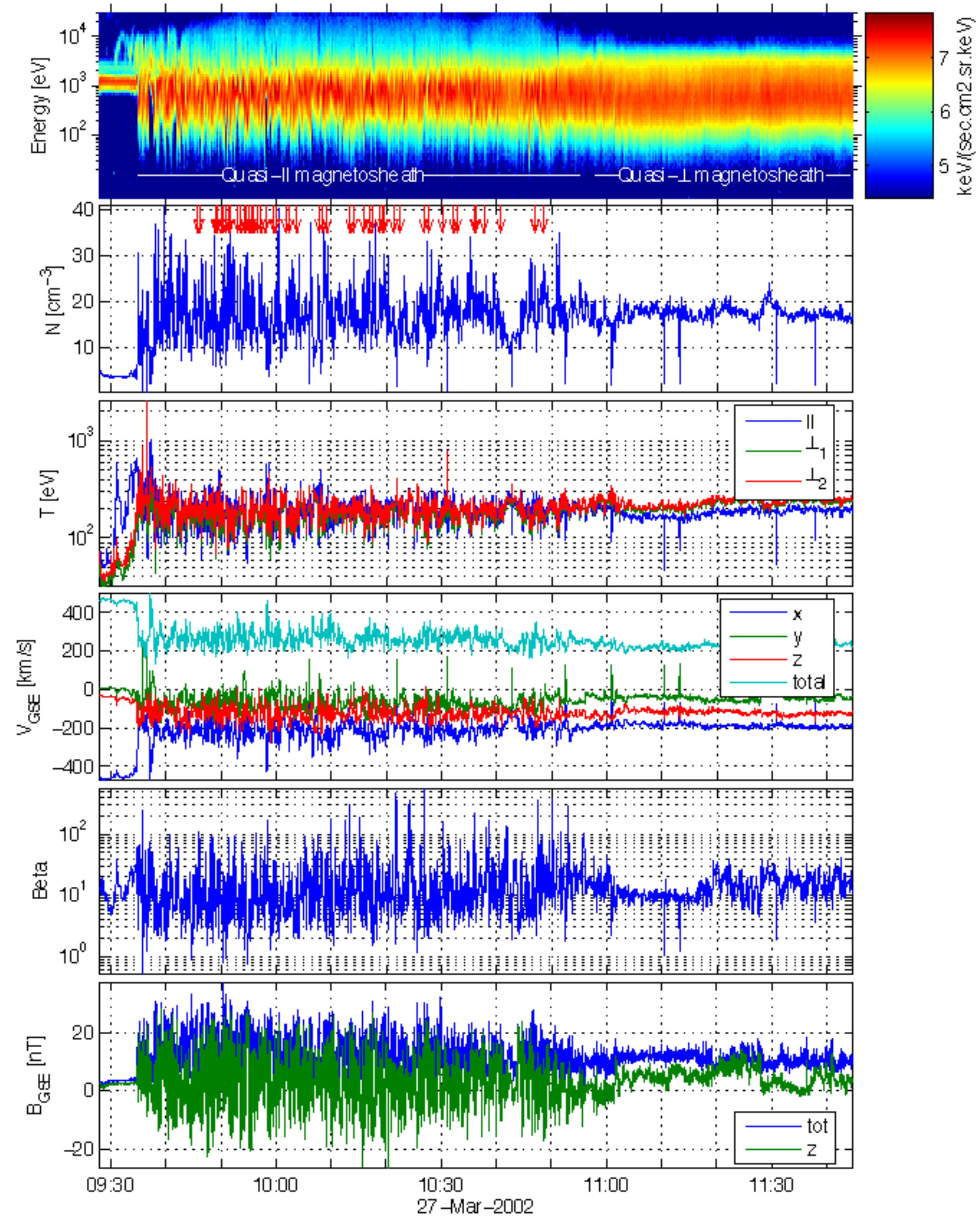

FIG. 1: Overview of plasma parameters in the outer magnetosheath as observed by Cluster spacecraft 1 (C1). **(a)** Ion spectrogram, **(b)** density, **(c)** ion temperature, **(d)** ion velocity, **(e)** plasma beta, **(f)** magnetic field. The occurence of thin current sheets for shear angle > 120 degrees is shown with arrows in panel b. See also Table (I).

small-scale current sheets

- a large fraction of the observed current sheets show evidence of reconnection
- another pathway to dissipation

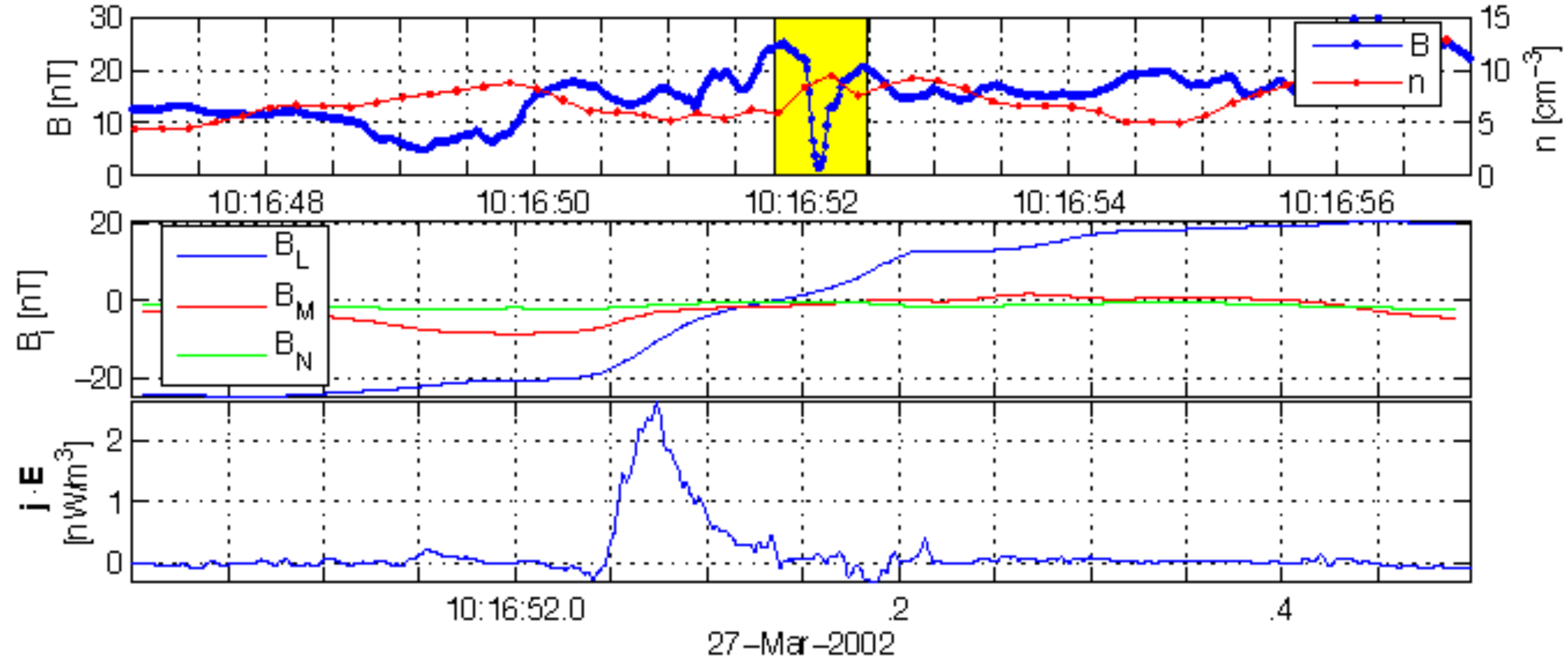

FIG. 2: Microphysics of a thin current sheet in the magnetosheath observed by C4. The LMN-coordinate system is defined in the text. **(a)** Magnetic field and density fluctuations. The yellow patch is shown in detail in panels (b) and (c). **(b)** Reconnecting component of magnetic field (B_L), out-of-plane component (B_M), normal component (B_N). **(c)** Dissipated power per unit volume.

(Sundkvist et al., PRL, 2006)

adiabatic motion, anisotropy, and instability

- particles streaming from the Sun should become focused if the motion is adiabatic
- if f(v) is isotropic near the Sun, it should be highly beamed at 1 AU
- highly anisotropic distribution functions are unstable to a variety of fluid and kinetic instabilities
- instabilities should scatter back towards isotropy

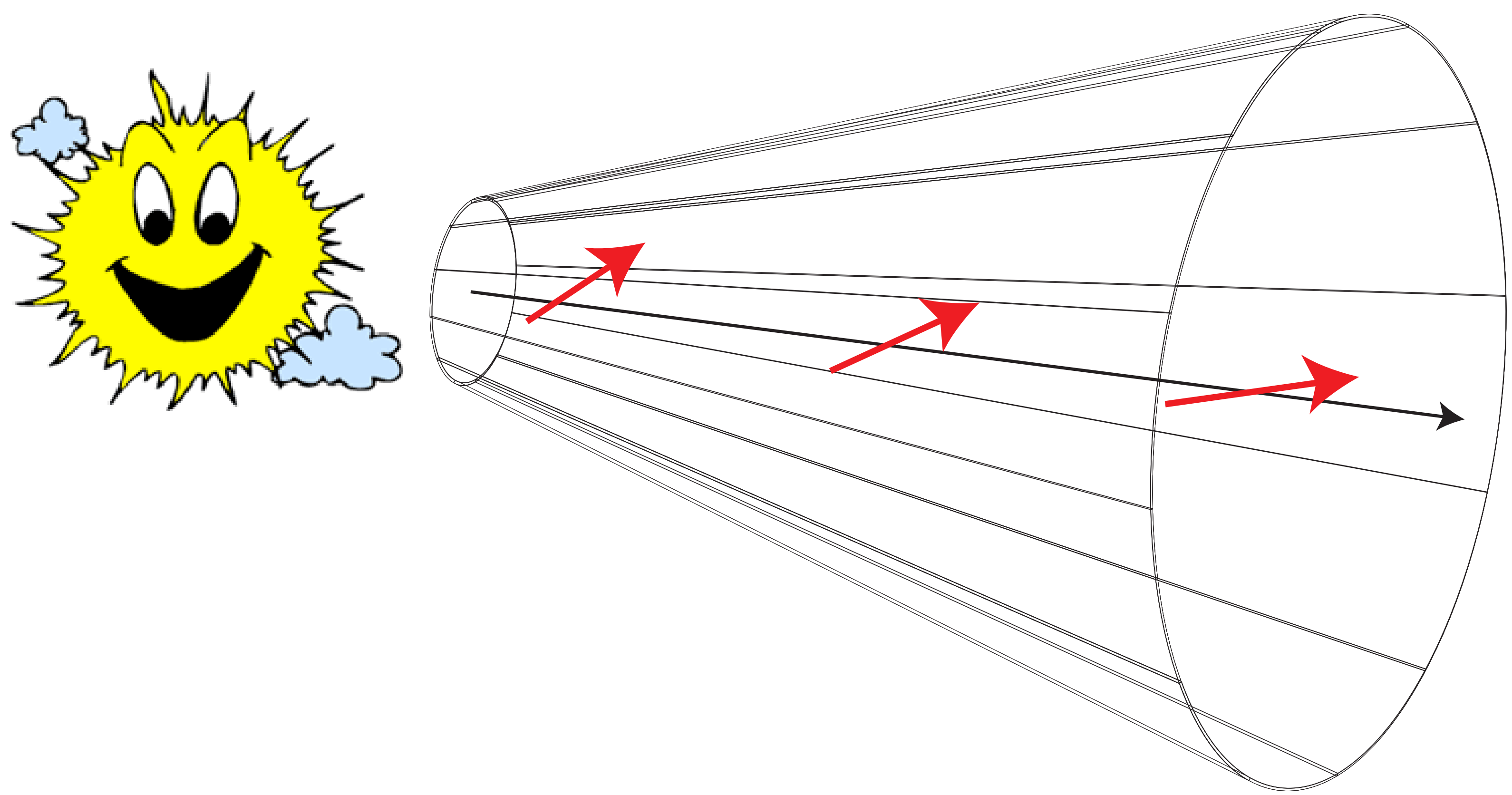

Wind spacecraft data analysis

We use Wind/MFI, SWE, and 3DP data - 10 years of virgin solar wind data (1M++ independent measurements), superior instrumentation, best time resolution, WAVES measurements

- Proton anisotropies from SWE - Kasper et al. dataset
- RMS magnetic fluctuation level during integration to 3 seconds
  - sampled onto timetags of Kasper et al. data
  - rotated to a field aligned coordinate system using 3 second averages
- Electron data from Wind/3DP EESA-L electrostatic analyzer
- Wind/WAVES is next...

anisotropic viscous stress

$$W_{r\phi} = -\left(1 - \frac{p_{\parallel} - p_{\perp}}{B^2}\right)\frac{B_r B_\phi}{4\pi} + \rho v_r \delta v_\phi$$

- can be comparable to the Maxwell stress in astrophysical plasmas
- results in ion and electron heating
- constrained by μ invariance and instabilities

proton temperature anisotropy

- Kasper et al. (GRL, 2002), Hellinger et al. (GRL, 2006)
- 10 years of Wind/SWE data
- proton anisotropy is bounded by the AIC and mirror and firehose instabilities
- are the waves there?

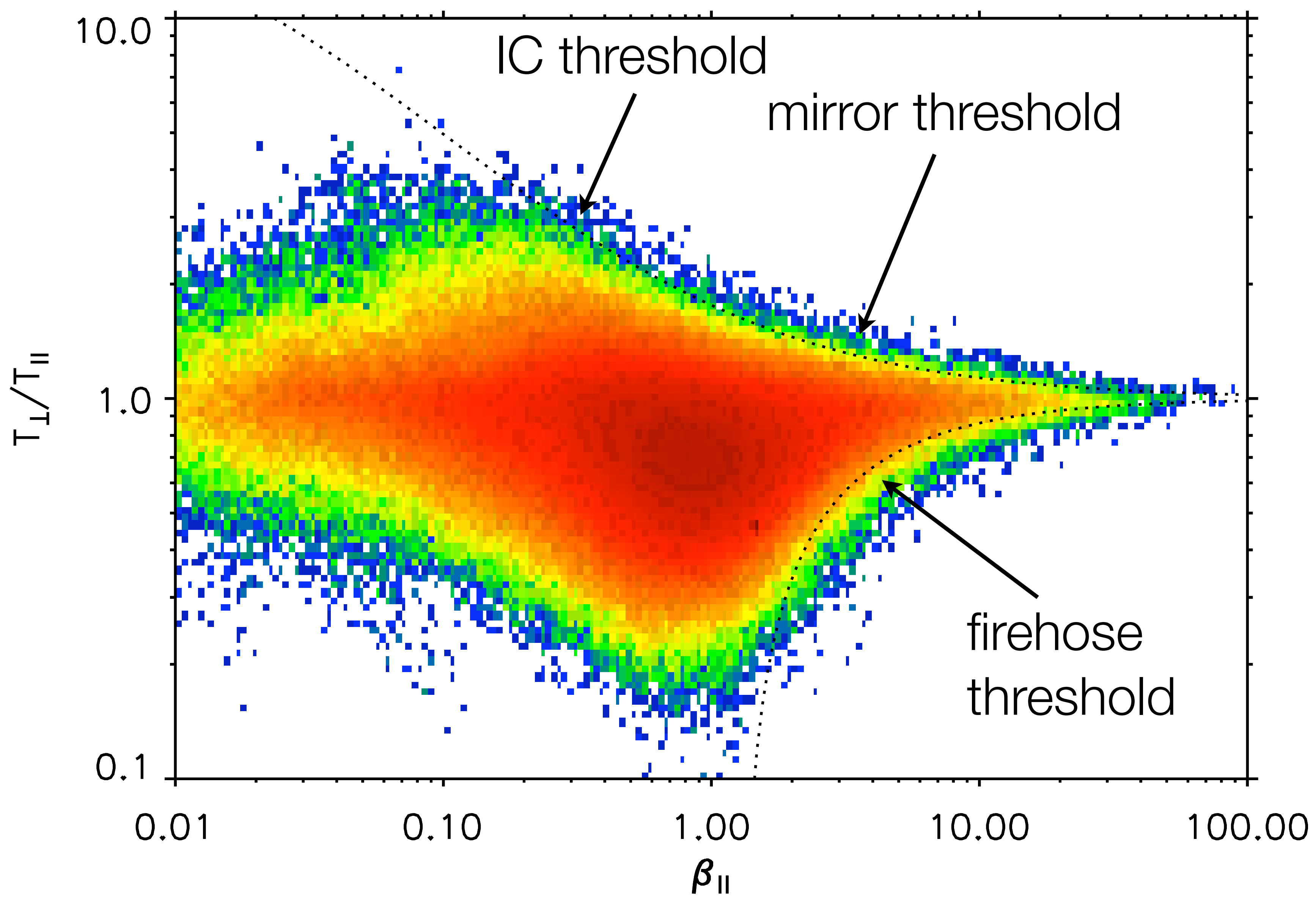

magnetic fluctuations

- magnetic fluctuation data sampled onto SWE (near-neighbor) timetags
- mapped into proton anisotropy-β space
- clear enhancements in fluctuation amplitude near both the oblique mirror and firehose threshold
- evidence of mirror-mode
- isotropic plasma is more collisional

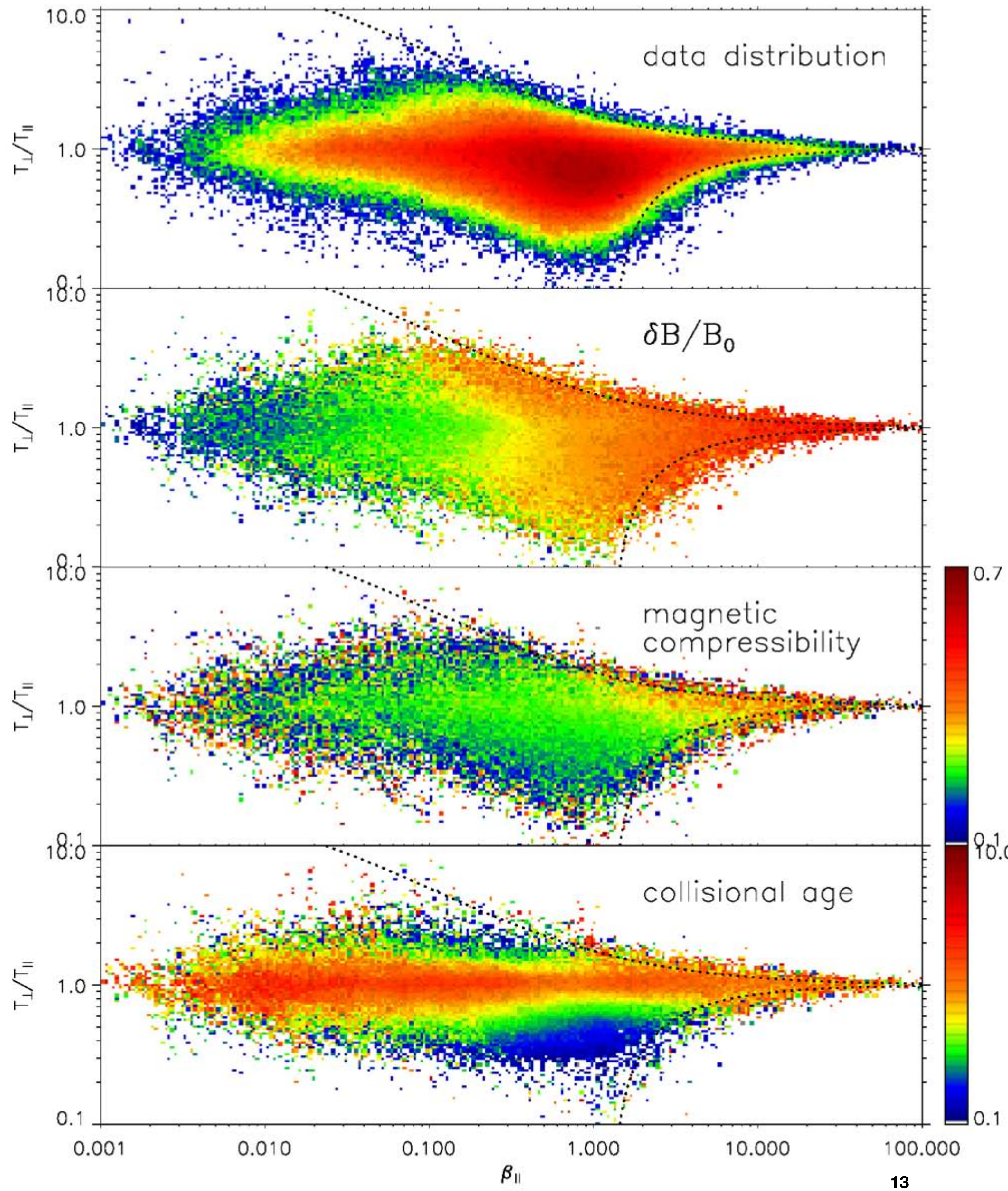

$\delta B/B$ vs $T_\perp/T_\parallel$ at β ~ 0.18

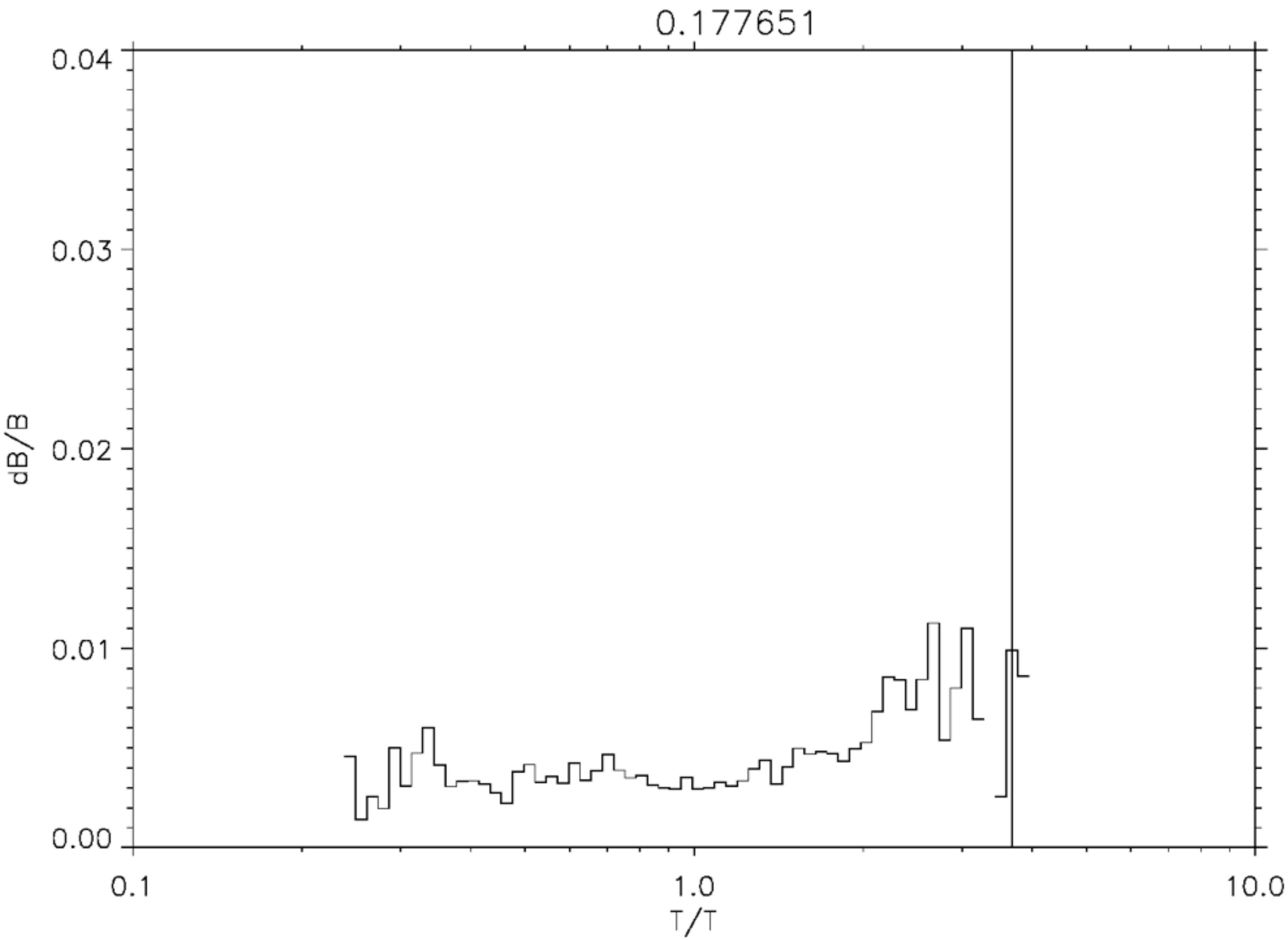

δB/B vs $T_\perp/T_\parallel$ at β ~ 0.35

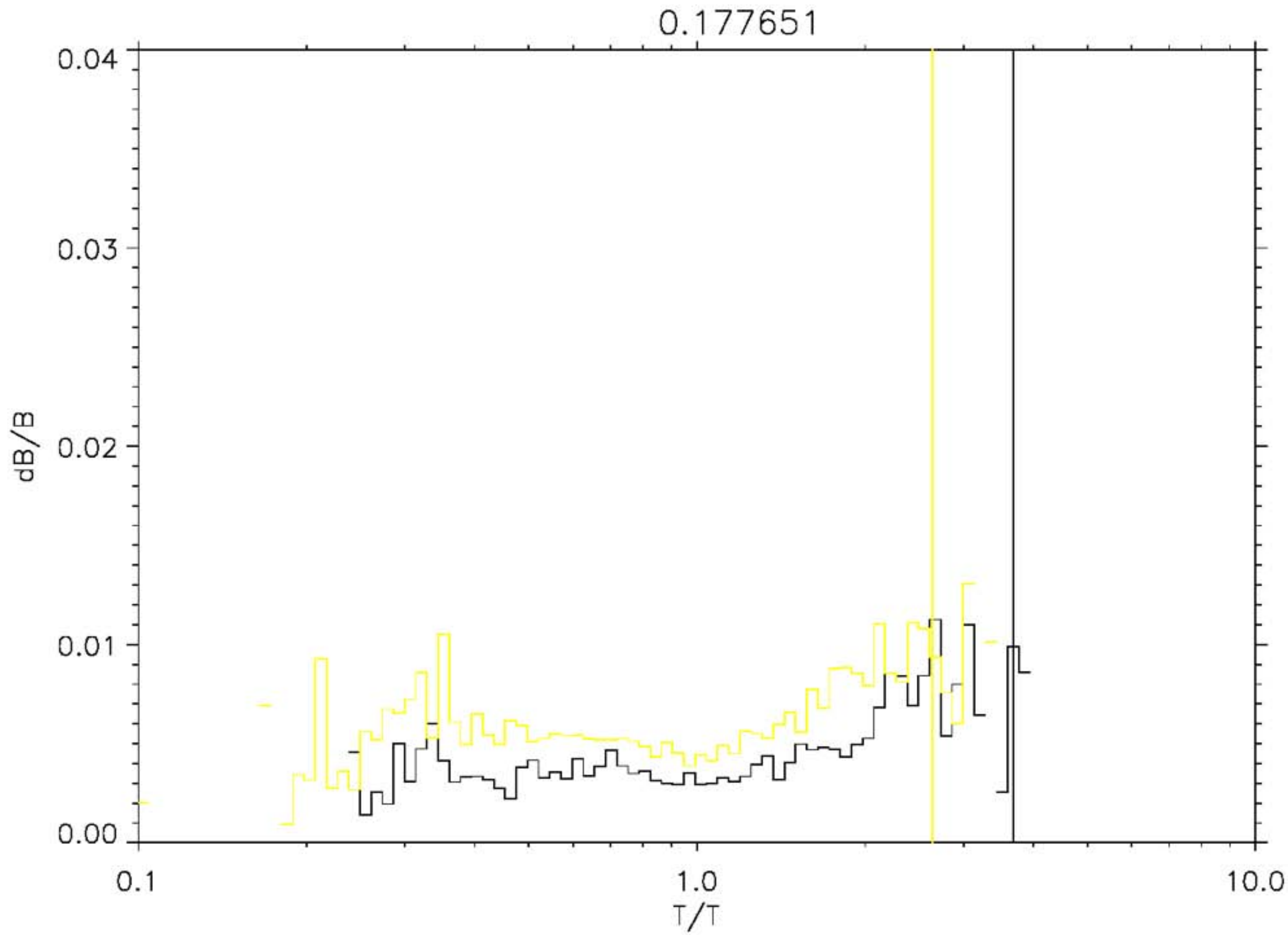

$\delta B/B$ vs $T_\perp/T_\parallel$ at β ~ 1.5

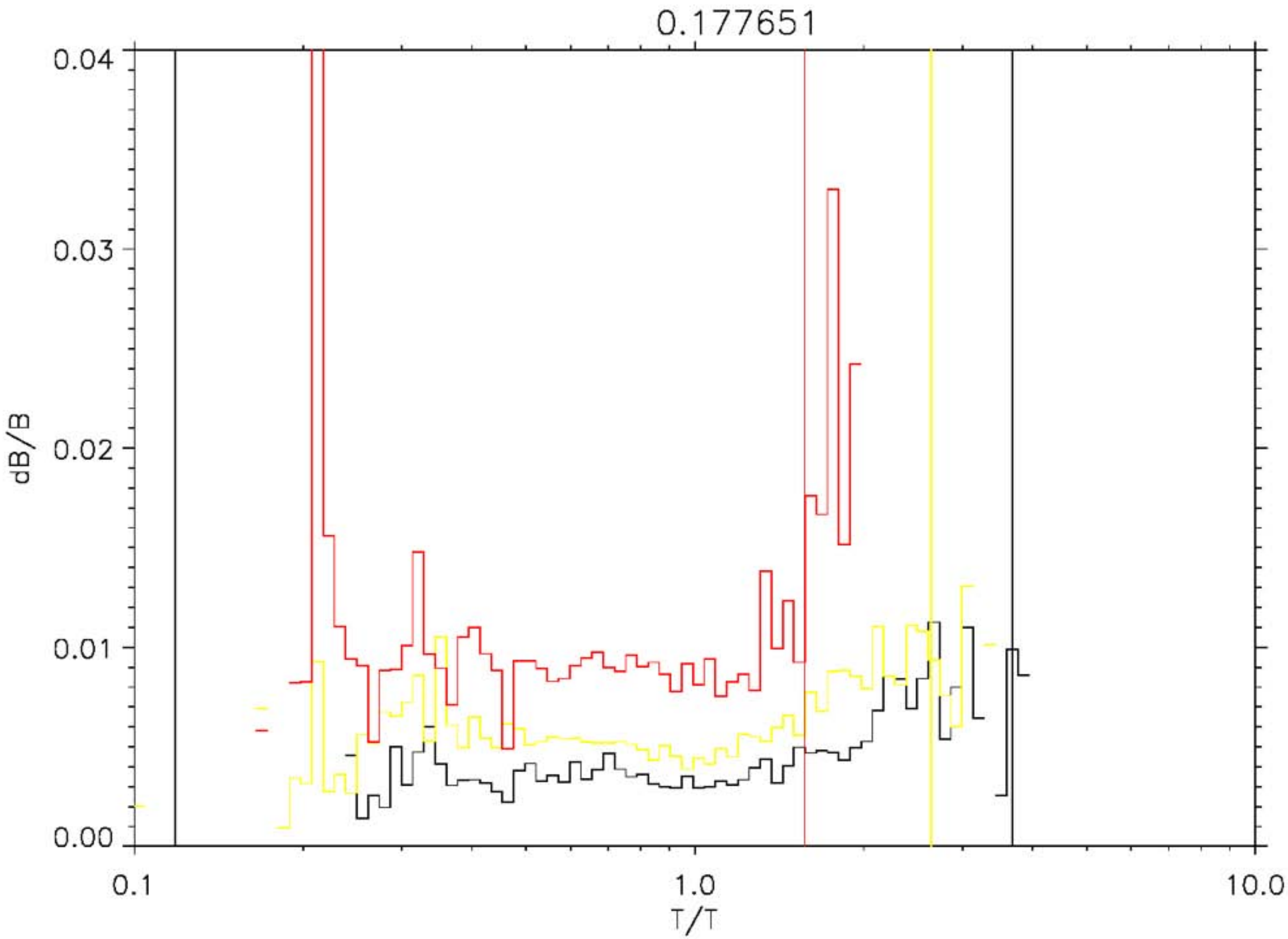

δB/B vs $T_\perp/T_{||}$ at β ~ 2.1

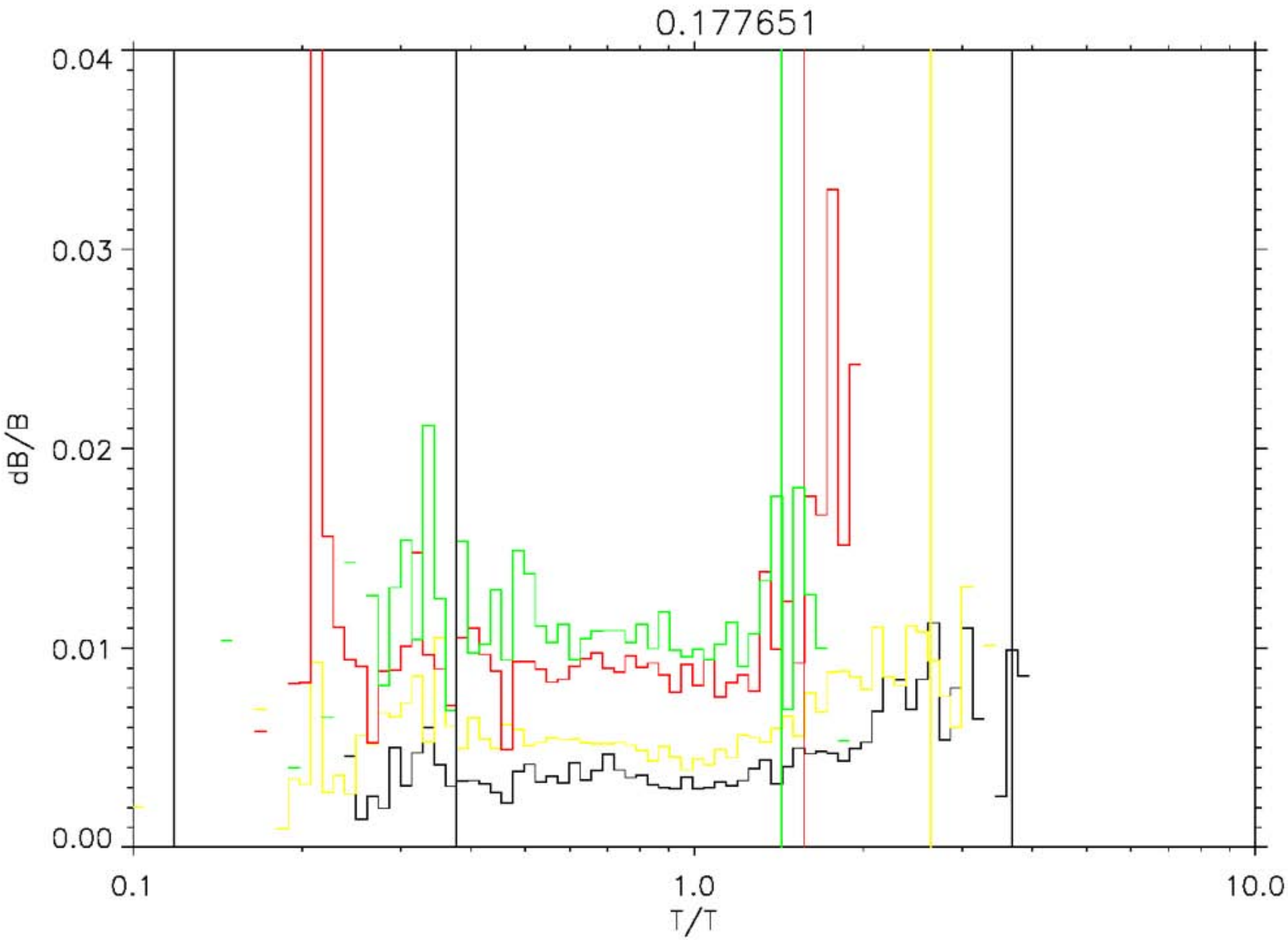

$\delta B/B$ vs $T_{\perp}/T_{||}$ at β ~ 4.1

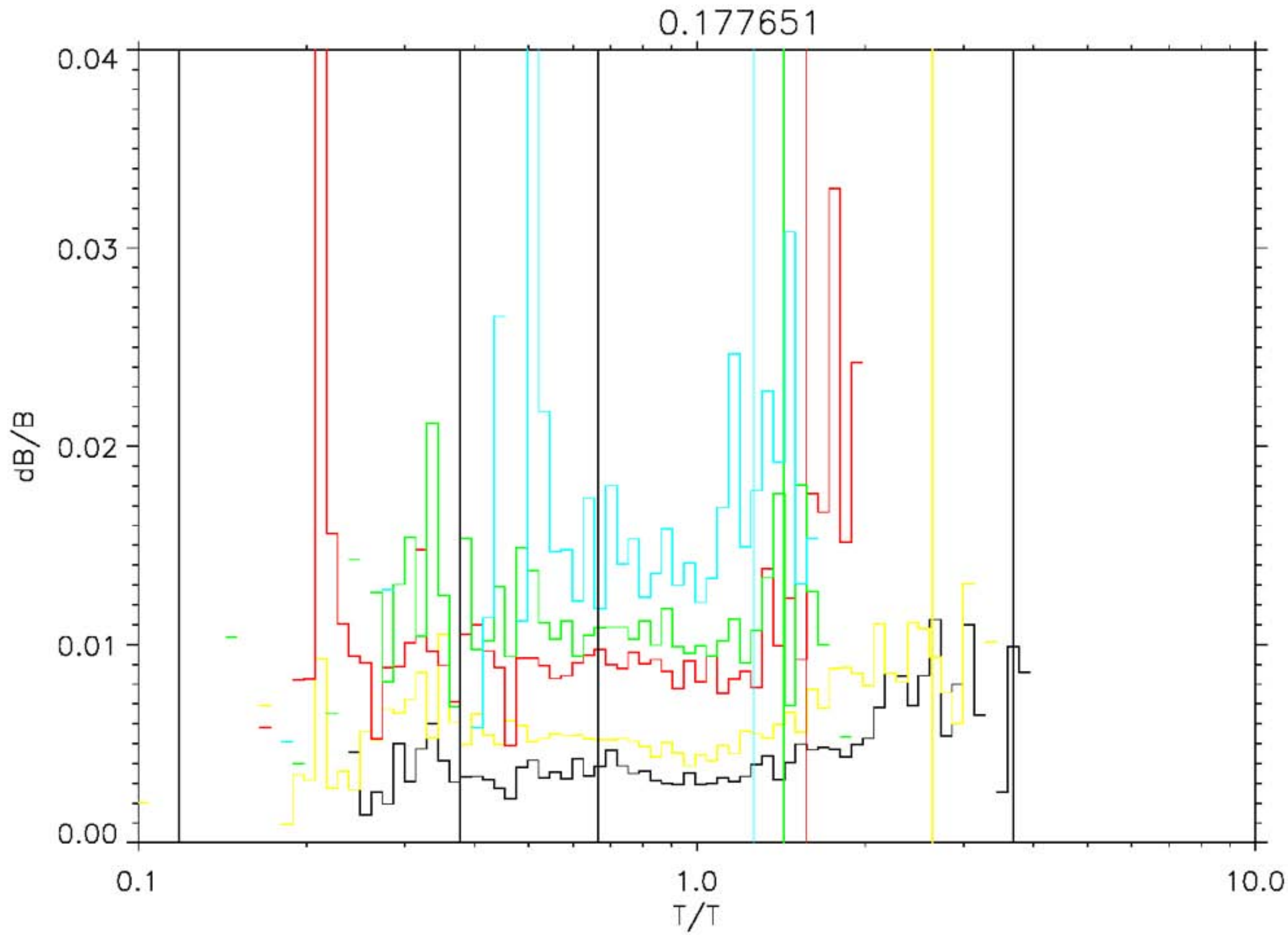

$\delta B/B$ vs $T_\perp/T_\parallel$ at $\beta \sim 7.1$

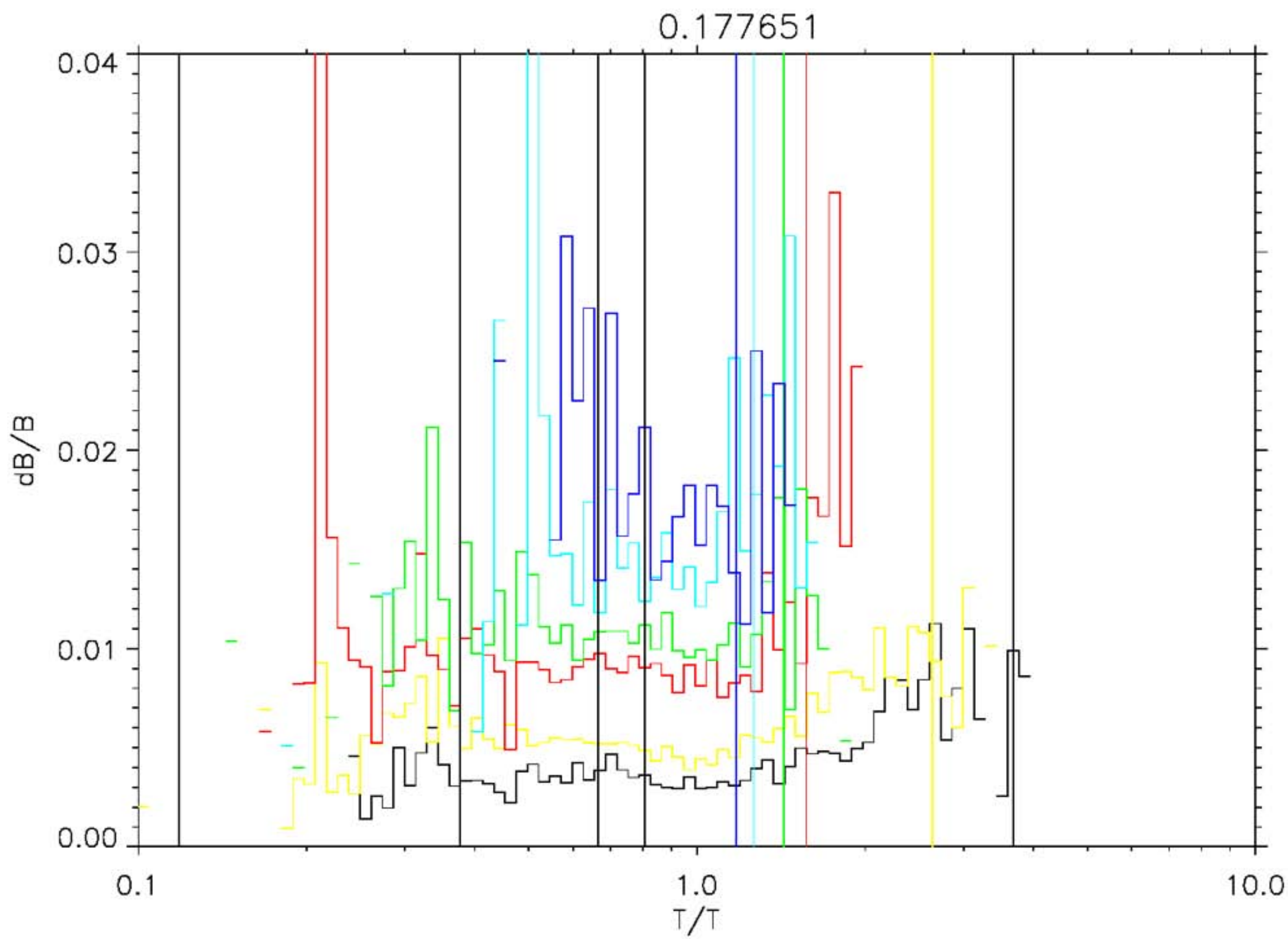

mirror mode has finite magnetic compressibility

linear mirror instability:

- zero frequency
- arbitrary k direction
- grows at finite perpendicular anisotropy
- large magnetic compression

$$\frac{b_{\parallel}^2}{b_{\parallel}^2 + b_{\perp}^2}$$

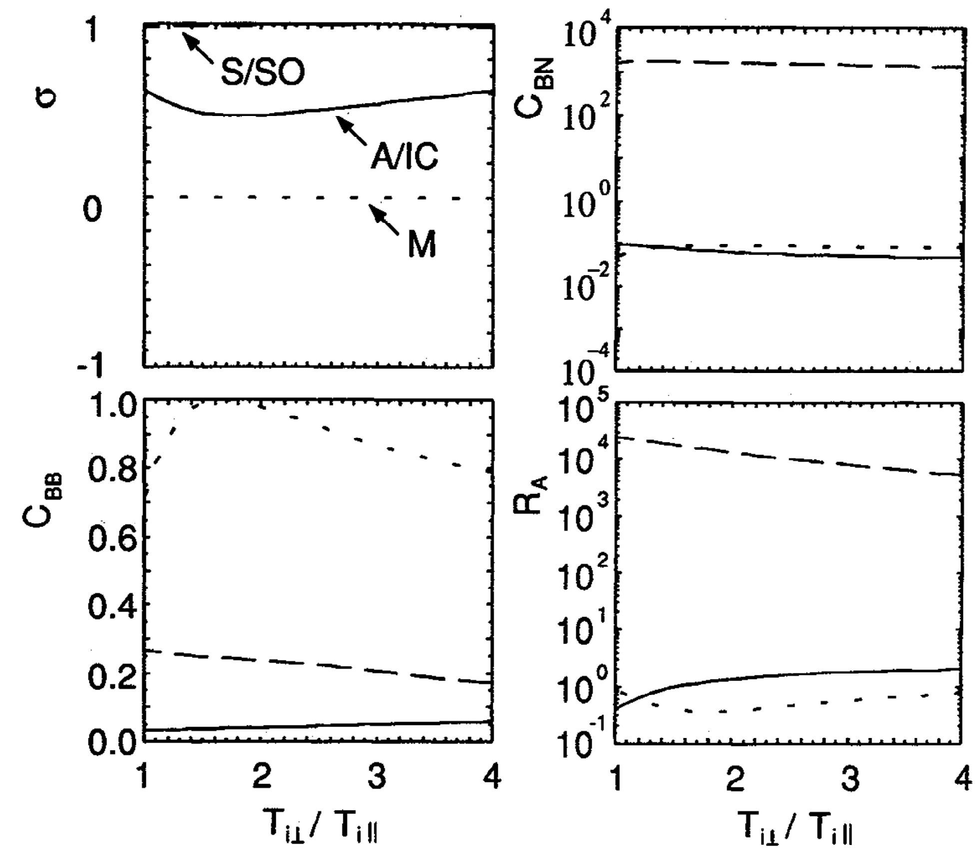

Figure 8b. Helicity σ, compressibility C_{Bn}, magnetic compression ratio C_{BB}, and Alfvén ratio R_A as a function of ion temperature anisotropy $T_{i\perp}/T_{i\parallel}$ for the same plasma conditions as in Figure 8a. The quantities shown are relatively insensitive to the anisotropy. When A/IC waves in both direction of propagation are present, σ does not allow to distinguish between the A/IC and M modes. Similarly, their values of C_{Bn} and R_A are fairly close. Also, R_A requires knowlegde of the perturbation velocity vector in observations (A14). Evidently, C_{BB} or a similar quantity based on the perturbation magnetic field direction is better suited to distinguish between these modes.

(Krauss-Varban et al., 1994)

measured magnetic compressibility

- magnetic fluctuation data sampled onto SWE (near-neighbor) timetags
- magnetic compressibility is computed $\frac{b_{\parallel}^2}{b_{\parallel}^2 + b_{\perp}^2}$
- mapped into proton anisotropy-β space
- clear enhancements in magnetic compressibility near the oblique mirror threshold for $\beta > 1$

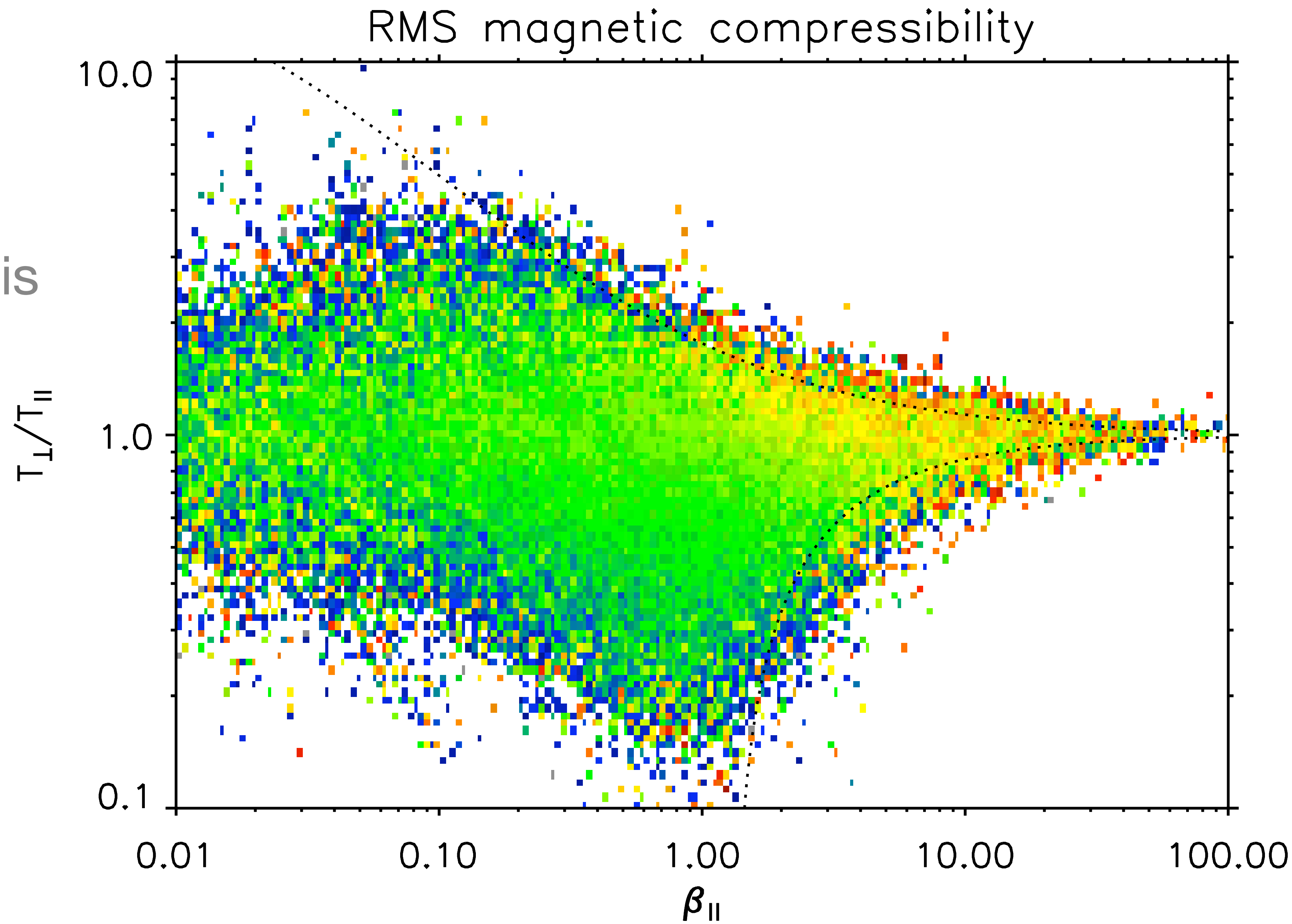

distribution of magnetic wave power

- magnetic fluctuation amplitude is non Gaussian: not Kolmogorov-like turbulence
- RMS power 1 sigma ~ 0.001 nT^2/Hz
- more power in perpendicular fluctuations (over entire dataset)

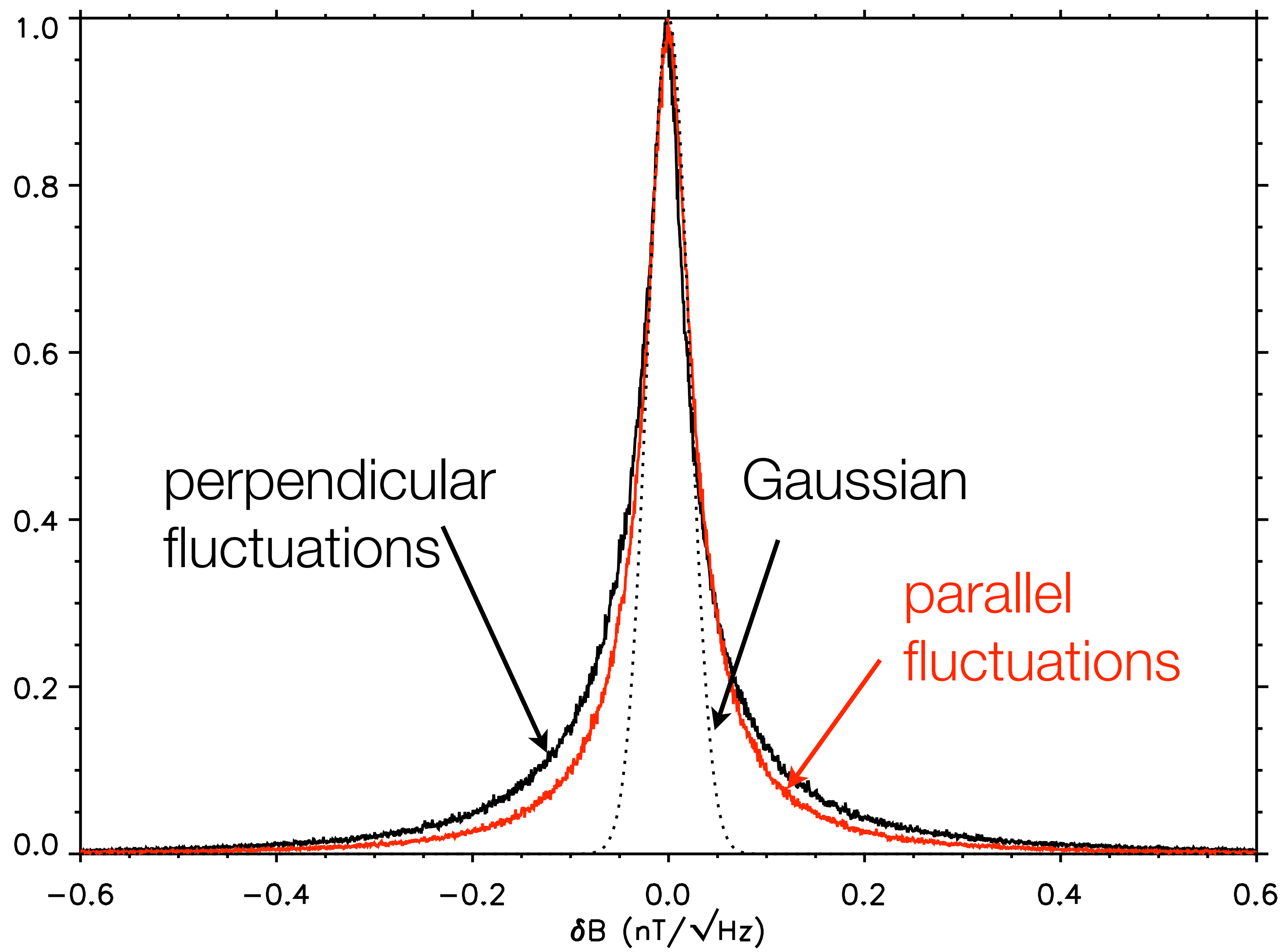

relationship to the magnetic fluctuation spectrum

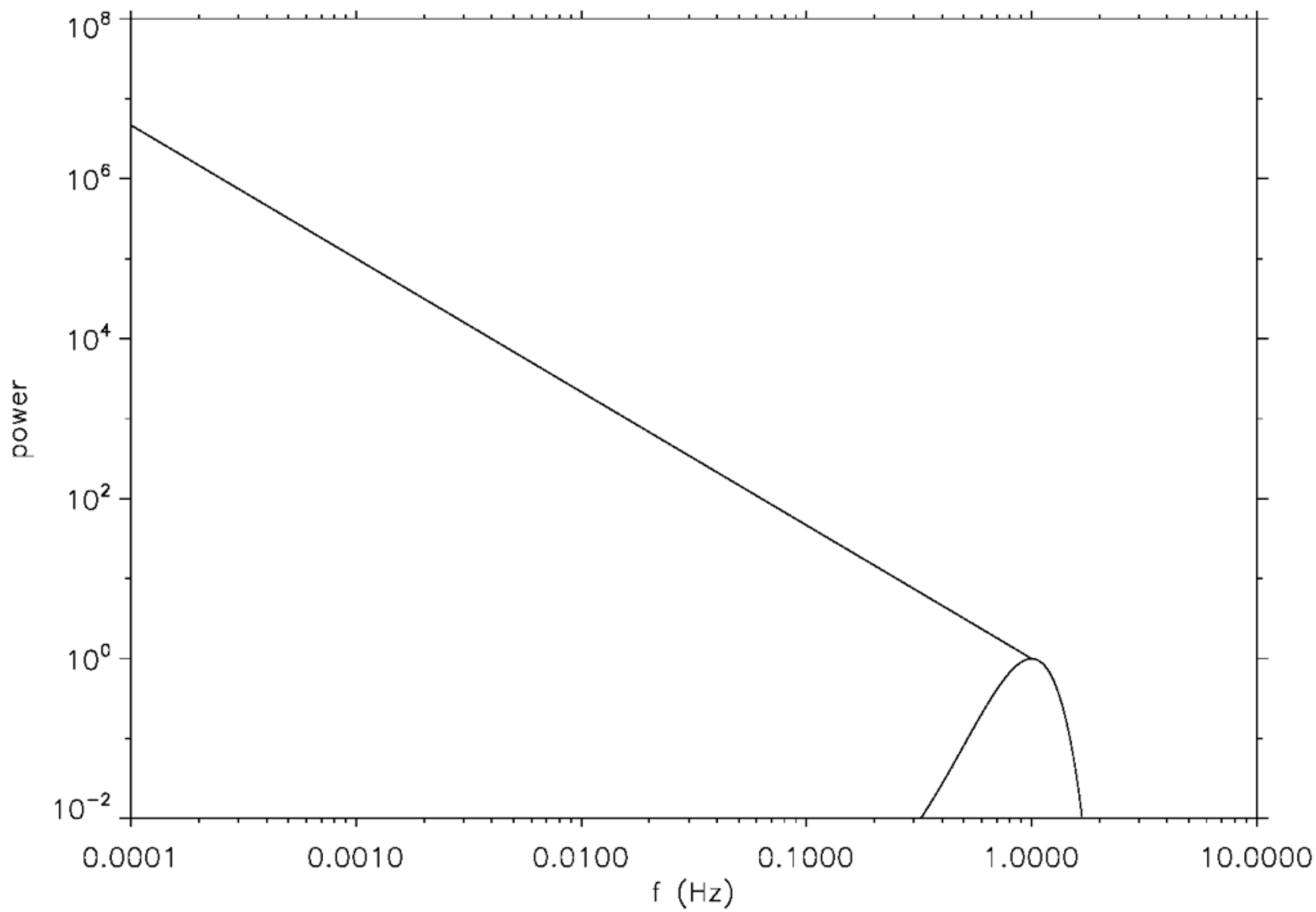

- instabilities should contribute to the power in the 'dissipation range'

relationship to the magnetic fluctuation spectrum

- black = isotropic, red = perp anisotropy, blue = parallel anisotropy
- white noise removed
- power at this intensity and bandwidth appears in the 'dissipation' (KAW) range
- any meaningful study of turbulent (wave-wave) dissipation must address the locally generated fluctuations

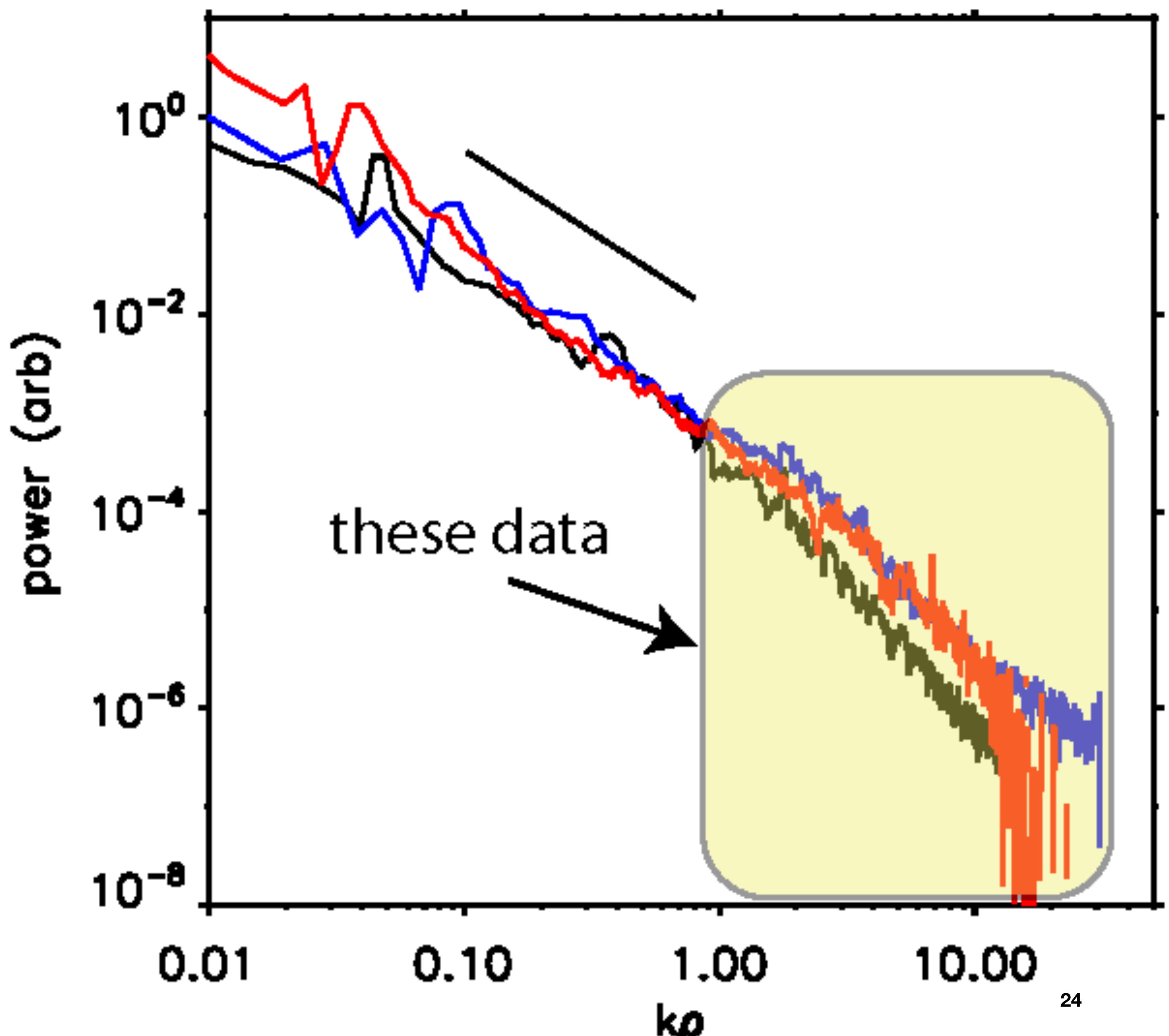

electron anisotropies

- Wind/3DP electron distributions at same time intervals as before
  ~ 1 million independent measurements
- corrected for spacecraft potential using SWE moments
- integrated into two populations:
  - core: 0 - 80 eV
  - halo: 80 - 1000 eV (anisotropy only)
- core is very isotropic - collisions
- halo is ordered by electron β

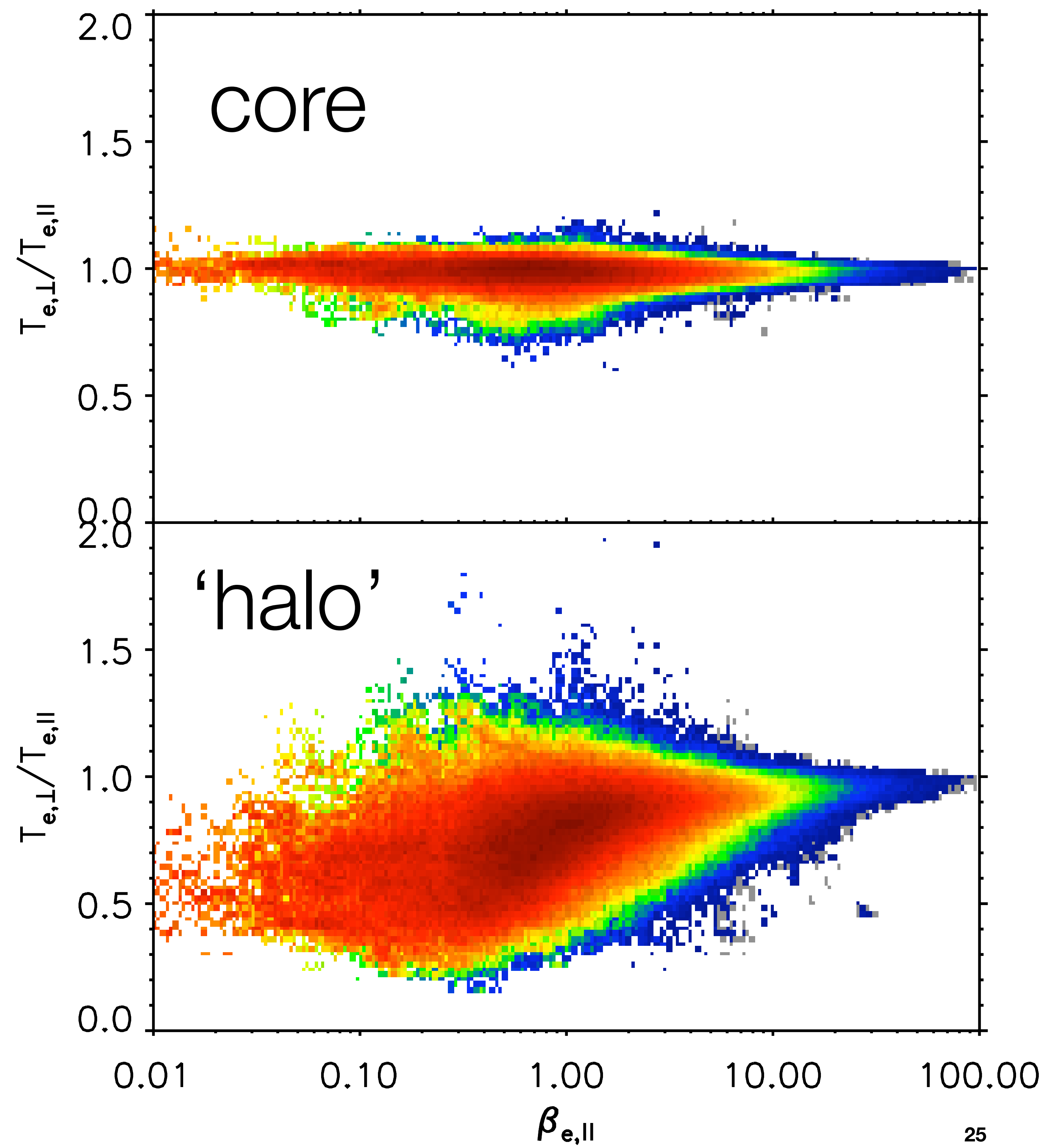

core anisotropy vs collisional age

- a 'collisional age' can be estimated from collision frequency and transit time (viz. Salem et al)
- core electrons appear to be well-ordered by collisions (here, at 1 AU)
- some anisotropy consistent with conservation of magnetic moment

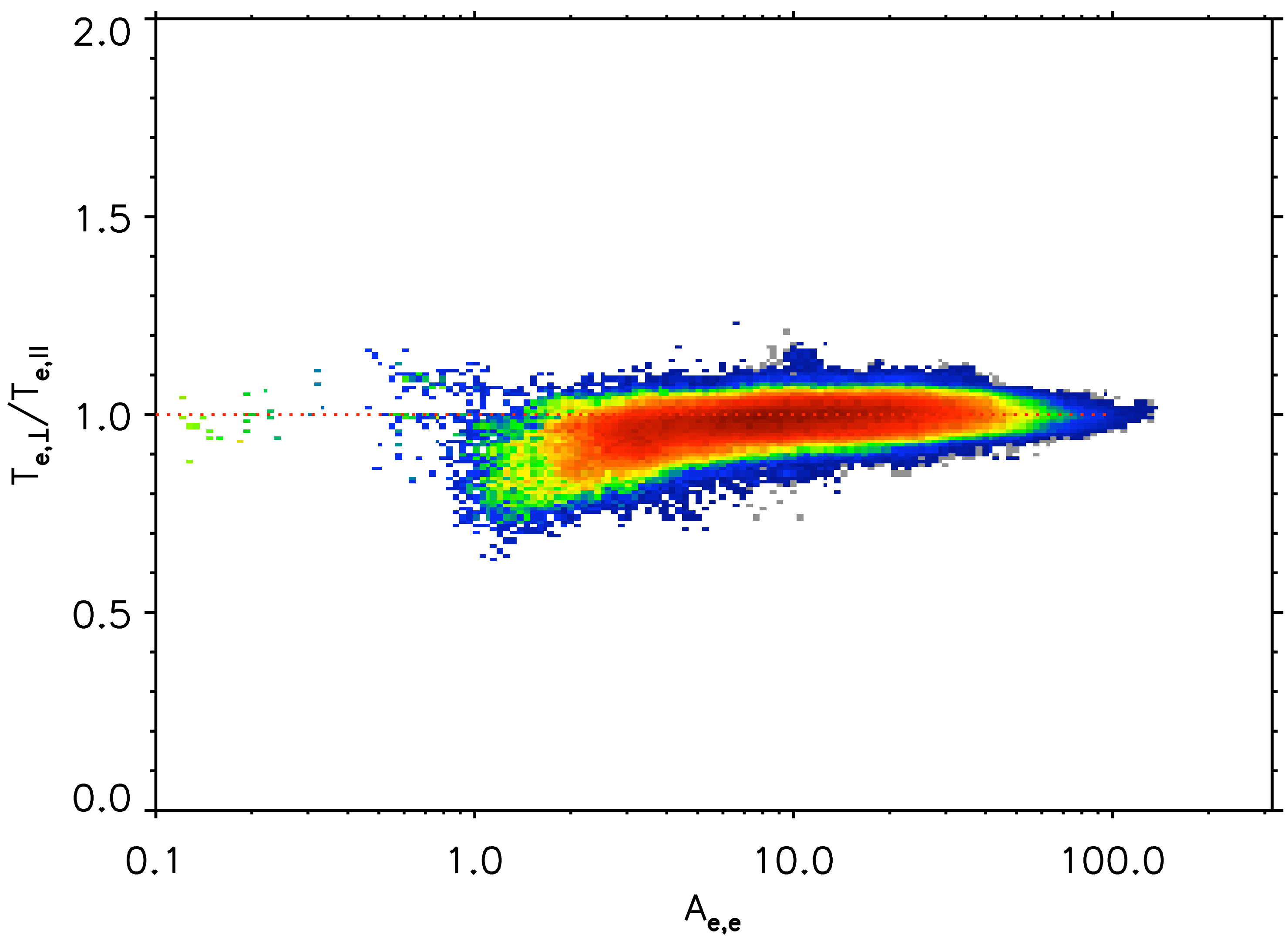

Halo anisotropies are constrained by instabilities

- halo is constrained by a whistler instability for $T_\perp/T_\| > 1$
- halo is constrained by the electron firehose instability for $T_\perp/T_\| < 1$

$$T_\perp/T_\| < 1 + S/\beta_{e,\|}^{\alpha}$$

	whistler		firehose	
count level	S	α	S	α
0.1%	0.275	0.577	-0.982	0.579
1%	0.147	0.647	-0.682	0.485
10%	-	-	-0.429	0.744

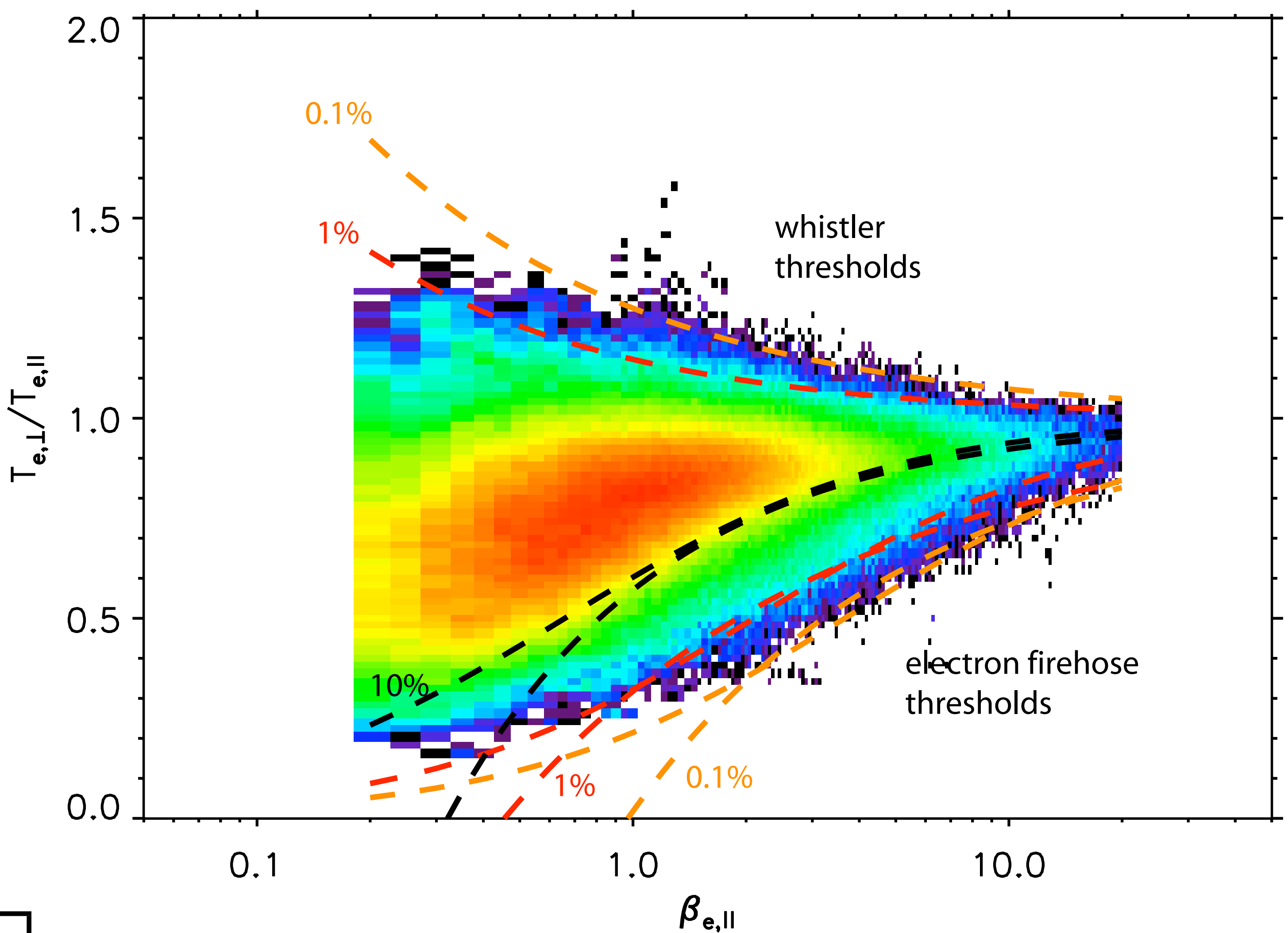

conclusions

- magnetic power around f_{ci} is enhanced near the proton mirror and firehose thresholds
- fluctuations near the mirror threshold show enhanced magnetic compressibility - further evidence of mirror
- these fluctuation should NOT be confused with wave-wave interactions of the turbulent Alfvenic/KAW cascade
- core electrons are dominated by collisions (as expected)
- halo electrons are constrained by the whistler and electron firehose instabilities (which should generate power near f_{ce})
- need electric field data!!

end